

Improvement of electron pump accuracy by a potential-shape-tunable quantum dot pumpMinky Seo,^{1,2,*†} Ye-Hwan Ahn,^{2,3,*} Youngeon Oh,¹ Yunchul Chung,^{1,‡} Sungguen Ryu,⁴ H.-S. Sim,⁴ In-Ho Lee,² Myung-Ho Bae,² and Nam Kim^{2,§}¹*Department of Physics, Pusan National University, Busan 609-735, Republic of Korea*²*Korea Research Institute of Standards and Science, Daejeon 305-340, Republic of Korea*³*Department of Physics, Korea University, Seoul 136-713, Republic of Korea*⁴*Department of Physics, Korea Advanced Institute of Science and Technology, Daejeon 305-701, Republic of Korea*
(Received 8 April 2014; revised manuscript received 18 July 2014; published 12 August 2014)

We have investigated the accuracy dependence of a single-electron pump on the confinement-potential shape of a quantum dot (QD) pump. A uniquely designed QD, which employs multiple gates to control the shape of the QD potential well, is utilized for electron pumping. It has been observed that the accuracy of the pump can be dramatically enhanced by achieving smaller QD size and greater decoupling from the electrodes, which is supported by the so-called decay-cascade model. The accuracy of the pump current is estimated, based on the decay-cascade model, to be close to 0.1 ppm for 80-pA pump current when the confinement-potential shape is optimally tuned. This is the highest reported accuracy, although it is a theoretically estimated value, among QD-based pumps measured at 4.2 K in the absence of an external magnetic field. Our numerical calculations show that the enhancement of the estimated accuracy is mainly due to the increase of the electron addition energy in the QD as well as the increase of the height and thickness of the QD potential barrier.

DOI: [10.1103/PhysRevB.90.085307](https://doi.org/10.1103/PhysRevB.90.085307)

PACS number(s): 73.23.Hk, 73.63.Kv

I. INTRODUCTION

Tunable-barrier electron pumps [1–7] have attracted considerable attention recently because of their potential application to the quantum current standard. Blumenthal *et al.* [1] demonstrated quantized current pumping up to 1 GHz by operating the gates of a quantum dot (QD) in a turnstile fashion. Following their study, it was reported that quantized current pumping could be achieved by modulating only a single gate of a QD: this is known as a “single-parameter charge pump” [3–5]. This technique is believed to be noteworthy progress towards the quantum current standard because multiple charge pumps can easily be parallelized for a scalable higher current output [8]. It has also been found that the pump-current accuracy can be significantly improved by modulating the pump with properly tailored wave forms under a high magnetic field [7,9,10]. The measured current accuracy was at least better than 1.2 ppm with an output current of 100 pA [7], which is very close to the requirement for fulfillment of the quantum metrology triangle [11].

In this work, we have employed a uniquely designed QD with a controllable confinement-potential shape, allowing it to function as a pump device. The confinement-potential shape of the QD is changed to study the effect on the pump-current accuracy. The accuracy of the pump current is theoretically estimated to be close to 0.1 ppm for a pumping frequency of 500 MHz when the confinement-potential shape is optimally tuned. The results are analyzed within a decay cascade model [7,12] to elucidate a possible mechanism responsible for the improved accuracy of the pump.

II. EXPERIMENTAL SETUP

Figure 1(a) shows a schematic diagram of our pump device. The device is fabricated on the surface of a 62-nm-deep two-dimensional electron gas (2DEG) wafer based on a GaAs/AlGaAs heterostructure with an electron density of $2.9 \times 10^{11} \text{ cm}^{-2}$ and a mobility of $2.5 \times 10^6 \text{ cm}^2 \text{ V}^{-1} \text{ s}^{-1}$ at a temperature of 4.2 K. Devices with two different sizes (75- and 50-nm-wide gate electrodes with a 75- and 50-nm gap between the gates, respectively) are fabricated. The devices show very similar characteristics. The devices are composed of three sets of split gates (entrance G_{ent} , plunger G_{p} , and exit gate G_{exit}) and one “trench” gate G_{T} placed in the gap of the split gates, as shown in Fig. 1(a).

Schematic potential diagrams showing the pumping mechanism [6,7,12,13] are presented in Fig. 1(b). A QD is formed by tuning the voltages V_{ent} , V_{p} , V_{exit} , and V_{T} on gates G_{ent} , G_{p} , G_{exit} , and G_{T} , respectively. The potential of the QD is varied periodically by modulating the entrance-gate voltage V_{ent} with rf biased. Electrons are loaded into the QD when the entrance barrier is below the Fermi energy E_{F} (red potential trace). As the barrier is lifted above E_{F} (blue potential trace), captured electrons in the QD start to tunnel back and escape from the QD. The accuracy of the pump current is mostly determined during this back-tunneling stage [6,7]. If the back-tunneling rate Γ_n of the n th electron is unity and the back-tunneling rates of the electrons below the n th states are zero, the pumped current will be $I = (n - 1)ef$, where e is the electron charge and f is the pumping frequency. Hence, the accuracy of the pump current is mostly determined by the ratio between Γ_n and Γ_{n-1} [6,7,12,13]. The ratio is known to depend mainly on two physical parameters, the thickness of the potential barrier of the QD and the electron addition energy ΔE of the QD; the latter is defined by $\Delta E = E_c + \delta E$, where E_c and δE are the charging energy e^2/C and energy-level spacing of the QD, respectively [6,10,12].

In our previous work, we reported that subband energy spacing in the quantum point contact (QPC) could be increased

*These authors contributed equally to the work.

†Present address: Department of Physics and Astronomy, Seoul National University, Seoul 151-747, Republic of Korea.

‡ychung@pusan.ac.kr

§namkim@kriss.re.kr

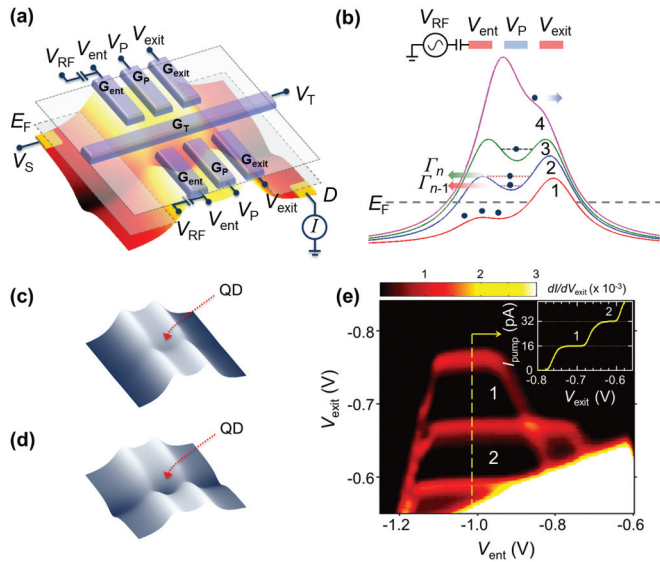


FIG. 1. (Color) (a) Schematic diagram of the device and the potential profile of the QD. Negative gate voltages V_{ent} , V_p , V_{exit} are applied on the entrance G_{ent} , plunger G_p and exit gates G_{exit} , respectively, while a positive V_T is applied on trench gate G_T to make the potential profile of the QD sharper and deeper. (b) Schematic potential diagram showing the pumping mechanism. V_{ent} is modulated periodically while V_p , V_{exit} , and V_T are fixed. Schematic diagrams of the potential profile of the QD with (c) zero voltage and (d) a positive voltage on G_T . The positive V_T makes the potential profile of the QD sharper and deeper. (e) Transconductance dI/dV_{exit} as a function of V_{exit} and V_{ent} , measured for $V_p = 0.375$ V, $V_T = 0.3$ V, $f = 100$ MHz, and $P_{RF} = 2$ dBm. The number on each plateau denotes the number of electrons pumped through the QD. Inset: the pump current I_{pump} measured along the dotted line ($V_{ent} = -1.01$ V).

by applying a positive voltage on a trench gate G_T placed in the gap of QPC split gates [14]. The maximum subband energy spacing was ~ 7 meV, which is much larger than that of a conventional QPC [15]. Taking a similar approach, the energy level spacing δE of a QD can be controlled by the trench-gate voltage V_T , as illustrated in Fig. 1(c) for zero and Fig. 1(d) for a positive V_T . As V_T increases, the shape of the QD potential well will be sharper and deeper to increase the energy-level spacing δE , which will eventually increase the electron addition energy ΔE of the QD. This scheme allows us to vary an important experimental parameter ΔE , which has not been explored in previously reported works [1–7].

All measurements are performed at 4.2 K in liquid helium without a magnetic field. Figure 1(e) shows a transconductance dI/dV_{exit} density plot obtained as a function of V_{ent} and V_{exit} for fixed values of V_p and V_T . The dark regions surrounded by the red boundaries correspond to the quantized current plateaus. The number on each plateau region denotes the number of electrons pumped through the QD from the source to the drain. The quantized currents as a function of V_{exit} [along the vertical dotted line in Fig. 1(e) for a fixed value of V_{ent}] are shown in the inset. This shows the current plateaus around integer multiples of 16 pA, which correspond to the expected currents nef (n is an integer number) with $f = 100$ MHz. The results are consistent with previously reported results [1–7].

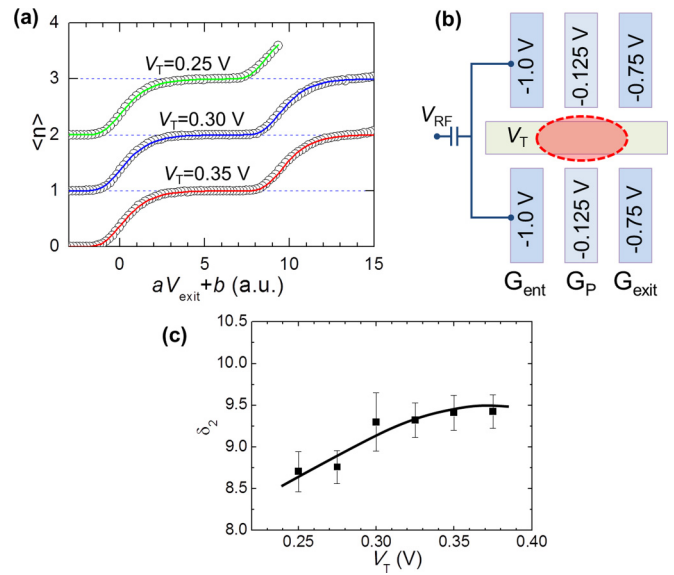


FIG. 2. (Color online) (a) Quantized pump currents measured for various values of V_T at $f = 100$ MHz with $P_{RF} = 2$ dBm, which are shifted in y axis for clarity. Open circles are measured currents normalized by ef as $\langle n \rangle_{exp} = I_{pump}/ef$. The x axis is rescaled to $aV_{exit} + b$, where a and b are fitting parameters. Solid lines are obtained by fitting the data to Eq. (1). (b) Each split gate is controlled separately, with the upper and lower parts of each split gate tied together as shown. A QD is expected to form symmetrically under G_T (marked as the red dashed line) since the gate voltages are applied symmetrically to the upper and lower parts of the split gates. The red dashed line is the schematic shape of the QD potential. (c) δ_2 vs V_T .

Note that our results are obtained at 4.2 K in the absence of an external magnetic field.

III. ELECTRON PUMPING

Figure 2(a) shows the first quantized current plateaus measured for various values of V_T with the other gate voltages tuned to form a QD as illustrated in Fig. 2(b), where the red dashed line represents the QD. Figure 2(a) reveals that the width of the first current plateau becomes wider as V_T increases. Since the pump-current accuracy is known to be proportional to the width of the current plateau [5], we can presume that the current accuracy can be improved by applying higher positive gate voltage on the trench gate G_T , which makes ΔE larger.

In order to estimate the current accuracy quantitatively from our data, we utilize a theoretical model, the so-called decay-cascade model proposed by Kashcheyevs *et al.* [6,12]. According to the model, the accuracy of the pump current is mostly determined at the back-tunneling stage, as illustrated in Fig. 1(b). For example, the pump current will be perfectly accurate when the back-tunneling rates $\Gamma_1 = 0$ (for the ground state) and $\Gamma_2 = \infty$ (for the first excited state). Thus, the ratio $\delta_2 = \ln(\Gamma_2/\Gamma_1)$ is considered an important figure of merit to determine the accuracy of the pump current [6,7]. The ratio δ_2 can be conveniently extracted by fitting the experimental data to the decay-cascade model. The analytic expression for the

pump current is given as follows:

$$\langle n \rangle_{\text{fit}} = \sum_{i=1}^2 \exp[-\exp(-aV_{\text{exit}} - b + \ln\Gamma_i)], \quad (1)$$

where Γ_i ($i = 1, 2$) is the back-tunneling rate of the i th electron in the QD and a and b are fitting parameters [7,12].

The ratio δ_2 is obtained by fitting our experimental data to Eq. (1). The extracted δ_2 values for various trench-gate voltages V_T are shown in Fig. 2(c). δ_2 shows a monotonic increase as a function of V_T [16], which is consistent with our assumption that a positive V_T makes the QD potential shape narrower and deeper, hence increasing the electron addition energy ΔE . Consider the back-tunneling rates Γ_1 and Γ_2 of electrons at the back-tunneling stage of trace 2 in Fig. 1(b). The potential barrier thickness experienced by an electron in the excited energy level E_2 becomes thinner compared to the case of the ground energy level E_1 when the addition energy $\Delta E = E_2 - E_1$ becomes larger. Consequently, $\delta_2 = \ln(\Gamma_2/\Gamma_1)$ is expected to be proportional to ΔE . It has to be mentioned that the entrance- and exit-gate voltages are retuned for new values of the trench-gate voltage, which in turn changes the barrier shapes of the entrance and exit potentials. However, the countercompensation of gate voltages, the tendency that the increase in the trench-gate voltage requires a decrease in the entrance- and the exit-gate voltage, keeps the barrier shapes rather unchanged for different values of the trench-gate voltage. Therefore, we believe that the enhancement of δ_2 is mostly due to the increase of the electron addition energy for the range of V_T varied in our experiment. The ratio δ_2 ranges from 8.5 to 9.6 depending on V_T . These values are slightly higher than those of QD pumps without a trench gate measured under similar conditions (zero external magnetic field, sinusoidal gate modulation, and liquid-helium temperature) [7,12].

Thus far we have studied the accuracy of the pump current when the QD is formed symmetrically (in shape) under the trench gate G_T , as shown in Fig. 2(b). However, it is found that δ_2 can be dramatically enhanced by forming the QD asymmetrically, as shown in Fig. 3(b). The same negative gate voltage (-0.66 V) is applied to all upper parts of the split gates to deplete the 2DEG in the upper region. A slightly positive voltage is applied to the lower part of the plunger gate G_P so that the QD is pushed towards the lower part of the plunger gate G_P , where the QD is represented as a red dashed line in Fig. 3(b) [17].

Figure 3(a) shows the measured quantized current steps when the QD is formed asymmetrically. Open circles are the experimental data, and the red line is the fitted result using Eq. (1) with $\delta_2 \sim 18$. The pump is modulated at a frequency of 500 MHz, which gives ~ 80 pA of single-electron pumping. The result is a dramatic enhancement over that measured for the symmetric QD case, where δ_2 is ~ 9 at 100 MHz and was reduced significantly at 500 MHz (not shown here).

The dependence of δ_2 on the pumping frequency is shown in Fig. 3(c). δ_2 is ~ 18 up to 500 MHz and linearly decreases above this frequency. The corresponding pump error ε_P , defined as $1 - \langle n \rangle_{\text{fit}}$ at the exit-gate voltage where $d\langle n \rangle_{\text{fit}}/dV_{\text{exit}}$ is locally minimized [6], is also plotted. For $\delta_2 = 18$, the pump error ε_P is close to 10^{-7} . For the symmetrical QD case, the pump error ε_P was $\sim 10^{-3}$ for measured $\delta_2 = 9$.

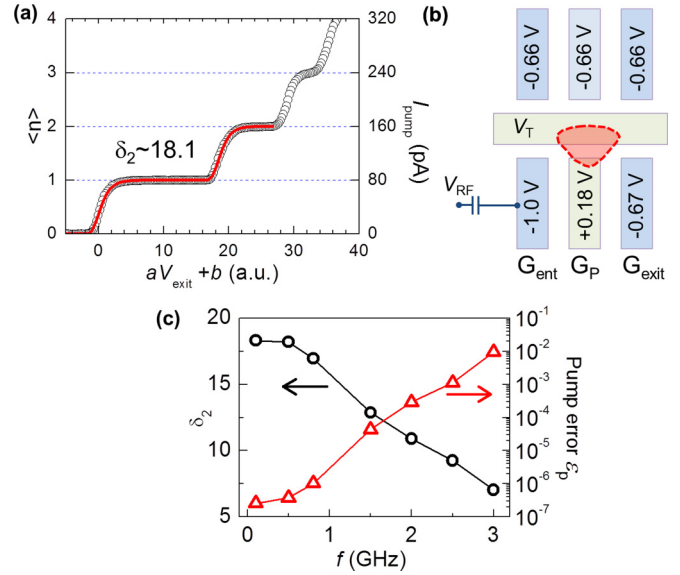


FIG. 3. (Color online) (a) Current normalized by ef measured (open circles) for $f = 500$ MHz and $P_{\text{RF}} = 2$ dBm when the QD is tuned asymmetrically as illustrated in (b). The solid line is $\langle n \rangle_{\text{fit}}$ with $\delta_2 \sim 18.1$. (b) The gate-voltage configuration to form an asymmetric QD (denoted as the red dashed line) for pumping. The rf signal is applied to the lower part of G_{ent} . The red dashed line is the schematic shape of the QD potential. (c) δ_2 (black circles) and ε_P (red triangles) as a function of f .

IV. NUMERICAL CALCULATIONS

To understand the dramatic enhancement of the pump-current accuracy for the asymmetric QD pump [18], $\delta_2 = \ln(\Gamma_2/\Gamma_1)$ is calculated fully quantum mechanically for both the symmetric and the asymmetric QDs, whose potential profiles were calculated by solving Laplace's equation analytically [19]. From the calculated QD confinement potential, the back-tunneling rates Γ_1 and Γ_2 are obtained by using the lattice Green's function method [10,20,21] and taking the imaginary part of the energy eigenvalues of the ground and excited states; the imaginary part appears because the effect of the semi-infinite leads is taken into account as the self-energy to the QD. Figures 4(a) and 4(b) are the potential profiles of the symmetric and asymmetric QDs, respectively, when the exit- and entrance-gate voltages are set to be equal. Figures 4(c) and 4(d) [4(e) and 4(f)] are the calculated local densities of states of the ground and first excited states for the potential profiles of Fig. 4(a) [Fig. 4(b)].

The calculated values of δ_2 are ~ 7.5 and ~ 5.5 for asymmetric and symmetric QDs, respectively, for various values of V_{ent} , as shown in Fig. 4(g). Even though the calculated δ_2 values are smaller than the experimental results and the enhancement of δ_2 for the asymmetric QD is not as significant as observed in the experiment, the results show qualitative agreement with the experimental results. The discrepancy between our analysis and the experimental result is due to the fact that our calculation has the following imperfections. First, electron-electron interactions are not taken into account. Our crude estimation of the charging energy E_c of the dot, based on dot size, indicates that E_c is roughly five times

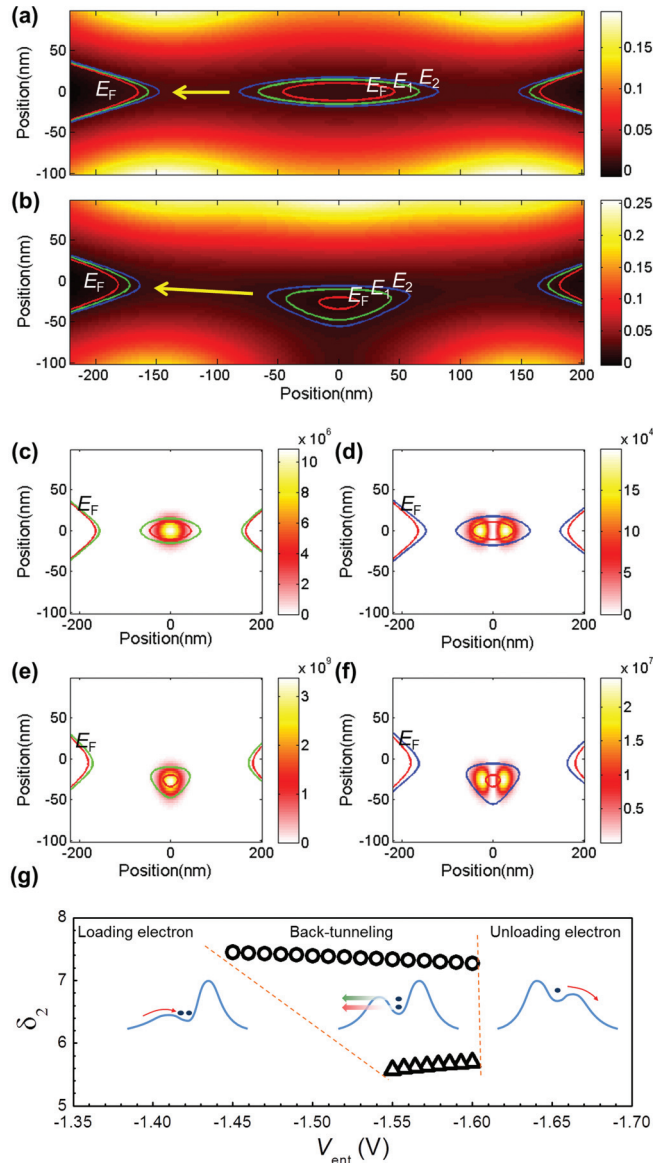


FIG. 4. (Color) The calculated potential profiles of the (a) symmetric and (b) asymmetric QDs around the center of the device. The energy levels E_1 , E_2 , and E_F of the ground (green lines), first excited (blue lines), and Fermi states (red lines), respectively, are calculated using the lattice Green's function method. The arrows indicate 1D tunneling trajectories with maximum tunneling probability. The calculated local density of states is shown for (c) and (e) the ground and (d) and (f) first excited states of the symmetric and asymmetric QDs, respectively. (g) The calculated δ_2 as a function of V_{ent} for the symmetric (open triangles) and asymmetric (open circles) QDs. δ_2 is calculated only for the case when both the ground and the first excited states are captured in the QD above E_F (i.e., during the back-tunneling stage). The dashed red lines show the boundaries between electron-loading, back-tunneling, and electron-unloading stages.

larger than the single-particle level spacing of the dot. Because of the interactions, more than the two lowest single-particle levels, within the energy window of E_c , contribute to Γ_2 . As a higher single-particle level has a larger back-tunneling rate, Γ_2 becomes larger as E_c increases. Therefore, the ratio

Γ_2/Γ_1 is underestimated in our calculation. As the charging energy of the asymmetric QD is roughly estimated as 1.2 times larger than that of the symmetric QD, the ratio Γ_2/Γ_1 is more underestimated for the asymmetric QD. Second, in our work, the QD potential is computed by solving Laplace's equations, following Ref. [19]. This approach is not accurate, however. To get a more accurate QD potential, the redistribution of two-dimensional electrons below the gates should be self-consistently treated. However, the self-consistent calculation of three-dimensional Poisson's equations is out of the scope of our study because it is extremely time-consuming. In addition, we do not take the spin degree of freedom into account. When a QD has two electrons, we need to consider the spin degree of freedom, hence spin-singlet and spin-triplet states. Because of the electron interaction (larger than single-particle level spacing), the two-electron ground state may favor a spin triplet; a spin-singlet state has a larger spatial overlap between the two electrons than a spin triplet, according to the Pauli exclusion principle; hence, it has a larger electron-electron interaction energy. For this reason, the ground state of the two electrons has a large probability that the two electrons have the same spin and each of the two lowest single-particle states is occupied by one electron [22]. Despite the imperfections, our analysis based on the back-tunneling rate of the two lowest single-particle states is qualitatively reasonable.

To determine the dominant physical parameters that contribute to the enhancement of δ_2 for the asymmetrical QD, we analyze the decay rate formula, $\Gamma_{1(2)} \propto \exp[-2d_{1(2)}\sqrt{2m^*(V_0 - E_{1(2)})}/\hbar]$, which is based on a one-dimensional (1D) WKB approximation [10,23]. Here, m^* is the effective electron mass, \hbar is Plank's constant divided by 2π , V_0 is the potential height, and $d_{1(2)}$ and $E_{1(2)}$ are the thickness of the potential barrier and the electron energy level corresponding to the ground state (1) and excited state (2) of the QD, respectively [24]. Under the limit $E_2 - E_1 \ll V_0$, $\delta_2 (= \ln\Gamma_2 - \ln\Gamma_1)$ is approximated as $\delta_{2,\text{WKB}} \approx \delta_{\Delta d} + \delta_{\Delta E}$, where $\delta_{\Delta d} = 2\sqrt{2m^*(V_0 - E_1)}/\hbar^2(-\Delta d)$, $\delta_{\Delta E} = d_1\sqrt{2m^*/\hbar^2}(V_0 - E_1)\Delta E$, $\Delta E = E_2 - E_1$, and $\Delta d = d_2 - d_1$. The physical factors affecting $\delta_{2,\text{WKB}}$ are therefore the disparity of the potential barrier thickness Δd , the addition energy ΔE , the thickness of the potential barrier d_1 , and the potential height $V_0 - E_1$. By analyzing each contribution of parameters ΔE , Δd , d_1 , and $V_0 - E_1$ to $\delta_{2,\text{WKB}}$ we can evaluate which physical factors are dominant. Our numerical analysis shows (detailed calculations are not shown here) that ΔE , d_1 , and $V_0 - E_1$ contribute almost equally to the enhancement of δ_2 in the asymmetric QD [in the pumping regime, for instance, $V_{\text{ent}} = -1.6$ to -1.55 V in Fig. 4(c)] [25].

One might expect that Δd also contributes to the enhancement of δ_2 because the difference in the values of Δd between the symmetric and asymmetric QDs could be significant. However, from our numerical results, the effect of Δd is estimated to be one order of magnitude smaller than the effects of the other parameters, including d_1 . Thus, we find that the increase of the addition energy by reducing the QD size and the increase of the barrier thickness by separating the QD from the electrodes are the origins of the enhancement of δ_2 in the asymmetric gate configuration. In other words, the physical factors such as the addition energy and the barrier thickness may not be directly related to the fact the QD shape

is asymmetric. The enhancement of δ_2 is merely the result of the fact that by pushing the QD to one side, a smaller and deeper dot with a thicker barrier can be created.

The ratio $\delta_2 \sim 18$, measured for the asymmetric QD configuration, is noticeable considering that the result is obtained at 4.2 K with the conventional sinusoidal rf modulation technique in the absence of a magnetic field. The result is comparable to the result reported by Giblin *et al.* [7], measured under a magnetic field of 14 T with a tailored rf wave-form modulation, a technique that is known to increase δ_2 significantly.

V. SUMMARY

We have demonstrated a type of single-electron pump that can tune the confinement-potential shape of a QD. It has been observed that the pump-current accuracy can be increased moderately by increasing the electron addition energy of the QD. A more dramatic enhancement of the current accuracy is

observed when the QD is formed asymmetrically in the pump. The theoretically estimated pump error is close to 10^{-7} for the asymmetric QD configuration, while the pump error for the symmetrical QD configuration is $\sim 10^{-3}$. Our work shows that the current accuracy of the single-electron pump can be increased by making a smaller QD or making a thicker and higher barrier between the QD and the electrodes.

ACKNOWLEDGMENTS

The authors are grateful to M. Kataoka for fruitful discussions. This work was supported by the Korea Research Institute of Standards and Science (KRISS). Y.C. was partially supported by the Basic Science Research Program through the National Research Foundation of Korea (NRF) funded by the Ministry of Education (Grant No. NRF-2013R1A1A2010792). H.S.S. was supported by the NRF (Grant No. NRF-2011-0022955).

-
- [1] M. D. Blumenthal, B. Kaestner, L. Li, S. Giblin, T. J. B. M. Janssen, M. Pepper, D. Anderson, G. Jones, and D. A. Ritchie, *Nat. Phys.* **3**, 343 (2007).
 - [2] A. Fujiwara, N. M. Zimmerman, Y. Ono, and Y. Takahashi, *Appl. Rev. Lett.* **84**, 1323 (2004).
 - [3] A. Fujiwara, K. Nishiguchi, and Y. Ono, *Appl. Phys. Lett.* **92**, 042102 (2008).
 - [4] B. Kaestner, V. Kashcheyevs, S. Amakawa, M. D. Blumenthal, L. Li, T. J. B. M. Janssen, G. Hein, K. Pierz, T. Weimann, U. Siegner, and H. W. Schumacher, *Phys. Rev. B* **77**, 153301 (2008).
 - [5] B. Kaestner, V. Kashcheyevs, G. Hein, K. Pierz, U. Siegner, and H. W. Schumacher, *Appl. Phys. Lett.* **92**, 192106 (2008).
 - [6] V. Kashcheyevs and B. Kaestner, *Phys. Rev. Lett.* **104**, 186805 (2010).
 - [7] S. P. Giblin, M. Kataoka, J. D. Fletcher, P. See, T. J. B. M. Janssen, J. P. Griffiths, G. A. C. Jones, I. Farrer, and D. A. Ritchie, *Nat. Commun.* **3**, 930 (2012).
 - [8] S. J. Wright, M. D. Blumenthal, M. Pepper, D. Anderson, G. A. C. Jones, C. A. Nicoll, and D. A. Ritchie, *Phys. Rev. B* **80**, 113303 (2009).
 - [9] S. J. Wright, M. D. Blumenthal, G. Gumbs, A. L. Thorn, M. Pepper, T. J. B. M. Janssen, S. N. Holmes, D. Anderson, G. A. C. Jones, C. A. Nicoll, and D. A. Ritchie, *Phys. Rev. B* **78**, 233311 (2008).
 - [10] J. D. Fletcher, M. Kataoka, S. P. Giblin, S. Park, H.-S. Sim, P. See, D. A. Ritchie, J. P. Griffiths, G. A. C. Jones, H. E. Beere, and T. J. B. M. Janssen, *Phys. Rev. B* **86**, 155311 (2012).
 - [11] M. W. Keller, F. Piquemal, N. Feltn, B. Steck, and L. Devoille, *Metrologia* **45**, 330 (2008).
 - [12] B. Kaestner, C. Leicht, V. Kashcheyevs, K. Pierz, U. Siegner, and H. W. Schumacher, *Appl. Phys. Lett.* **94**, 012106 (2009).
 - [13] M. Kataoka, J. D. Fletcher, P. See, S. P. Giblin, T. J. B. M. Janssen, J. P. Griffiths, G. A. C. Jones, I. Farrer, and D. A. Ritchie, *Phys. Rev. Lett.* **106**, 126801 (2011).
 - [14] Y. J. Um, Y. H. Oh, M. Seo, S. Lee, Y. Chung, N. Kim, V. Umansky, and D. Mahalu, *Appl. Phys. Lett.* **100**, 183502 (2012).
 - [15] K. J. Thomas, M. Y. Simmons, J. T. Nicholls, D. R. Mace, M. Pepper, and D. A. Ritchie, *Appl. Phys. Lett.* **67**, 109 (1995).
 - [16] When V_T is increased in the positive direction, it is necessary to set the rest of the gate voltages to more negative values in order to observe the quantized current.
 - [17] The 2DEG under the lower plunger gate G_p is still depleted due to large negative voltages on the entrance gate G_{em} and the exit gate G_{exit} .
 - [18] Three different samples were measured, and all of them show almost two times larger values of δ_2 for the asymmetric QD configuration than for the symmetric QD configuration.
 - [19] J. J. Davies, I. A. Larkin, and E. V. Sukhorukov, *J. Appl. Phys.* **77**, 4504 (1995).
 - [20] H.-S. Sim, G. Ihm, N. Kim, and K. J. Chang, *Phys. Rev. Lett.* **87**, 146601 (2001).
 - [21] S. Datta, *Electronic Transport in Mesoscopic Systems* (Cambridge University Press, Cambridge, 1997).
 - [22] We note that when the electron interaction energy is smaller than the single-particle level spacing, the ground state will be in a spin-singlet state in the absence of an external magnetic field and in a spin-triplet state under a strong magnetic field (under which the interaction energy is enhanced), as reported in L. P. Kuowenhoven *et al.*, *Science* **278**, 1788 (1997).
 - [23] Rudolph E. Langer, *Phys. Rev.* **51**, 669 (1937).
 - [24] The chosen 1D trajectory is the line of the maximum back-tunneling probability, denoted by arrows in Figs. 4(a) and 4(b). $d_{1(2)}$ is determined from the 1D path that gives the highest tunneling probability between the energy level $E_{1(2)}$ and the source electrode in the 2D energy contour, as shown in Figs. 4(a) and 4(b).
 - [25] Even though $\delta_{2,WKB}$ obtained from the 1D WKB method is slightly different from the δ_2 values obtained from the fully 2D Green's function method, the ratio of δ_2 between the symmetric and the asymmetric QDs, $\gamma = \delta_{2,asym}/\delta_{2,sym}$, is quite consistent between the 1D WKB method and the fully 2D Green's function method; for instance, $\gamma_{Green} \sim 1.3$ and $\gamma_{WKB} \sim 1.4$. Thus, our analysis based on the 1D WKB approximation is quite reasonable.